Optothermally actuated capillary burst valve

Eriksen, Johan; Bilenberg, Brian; Kristensen, Anders; Marie, Rodolphe

Published in:
Review of Scientific Instruments

Link to article, DOI:
10.1063/1.4979164

Publication date:
2017

Document Version
Publisher's PDF, also known as Version of record

Optothermally actuated capillary burst valve

Johan Eriksen, Brian Bilenberg, Anders Kristensen, and Rodolphe Marie

Citation: Review of Scientific Instruments **88**, 045101 (2017); doi: 10.1063/1.4979164
View online: http://dx.doi.org/10.1063/1.4979164
View Table of Contents: http://aip.scitation.org/toc/rsi/88/4
Published by the American Institute of Physics

Optothermally actuated capillary burst valve

Johan Eriksen,[1] Brian Bilenberg,[2] Anders Kristensen,[1] and Rodolphe Marie[1,a)]
[1]*DTU Nanotech, Technical University of Denmark, Oersted Plads, Building 345C, DK-2800 Kongens Lyngby, Denmark*
[2]*NIL Technology ApS, DK-2800 Kongens Lyngby, Denmark*

(Received 29 November 2016; accepted 14 March 2017; published online 3 April 2017)

We demonstrate the optothermal actuation of individual capillary burst valves in an all-polymer microfluidic device. The capillary burst valves are realised in a planar design by introducing a fluidic constriction in a microfluidic channel of constant depth. We show that a capillary burst valve can be burst by raising the temperature due to the temperature dependence of the fluid surface tension. We address individual valves by using a local heating platform based on a thin film of near infrared absorber dye embedded in the lid used to seal the microfluidic device [L. H. Thamdrup *et al.*, Nano Lett. **10**, 826–832 (2010)]. An individual valve is burst by focusing the laser in its vicinity. We demonstrate the capture of single polystyrene 7 μm beads in the constriction triggered by the bursting of the valve.
[http://dx.doi.org/10.1063/1.4979164]

INTRODUCTION

Microfluidics enables the manipulation of single particles. The architecture of microfluidics channels become more complex as parallelization increases and more functionalities are integrated, so that microfluidic systems require valves. State-of-the-art microfluidic devices using an external pressure source such as platforms for a single cell analysis are based on the pneumatic valve.[1] The pneumatic valve is realised by using a lid comprising an elastomeric layer that deforms under air pressure and collapses into the microfluidic channel. The architecture allows a high device complexity; however, there is an interest for valves without moving parts so that single use devices can be fabricated in thermoplastic materials with scalable industrial processes. Such valves are extensively used in centrifugal microfluidics where no external pressure source is used so that many active and passive valves have been implemented.[2,3] In this context, capillary burst valves (CBV) are attractive since the bursting pressure depends solely on the device geometry and the liquid properties.[4] In a capillary burst valve, the air-liquid meniscus is pinned by an abrupt change of geometry in a microfluidic channel. In its simplest form, the capillary burst valve is applied for windowless microfluidics[5] or filling complex microfluidic networks;[6,7] however it is in capillary microfluidics[8] and centrifugal microfluidics[9] that capillary burst valves play a central role. A valve can be predictably burst by increasing the centrifugal force above a threshold that depends mainly on its position on the rotating disc as well as on the length of the liquid column and the density of the liquid. This is convenient; however design flexibility can be increased if an actuation mechanism is introduced. The theory behind the capillary burst valve predicts that the bursting pressure depends on the surface tension of the liquid; thus a capillary burst valve can be thermally actuated. We first demonstrate thermal actuation by raising the temperature of the whole device. We then demonstrate an optically actuated capillary burst valve combining a local heating platform with a simple capillary burst valve design. Thambrup *et al.* have shown optically induced local heating using a near-infrared absorbing layer embedded in the lid of a microfluidic channel.[10] Conveniently, the optothermal platform is based on an external laser so that the actuation of the capillary burst valve does not complicate the microfluidic system itself. Optical actuation can easily be integrated in a centrifugal microfluidics platform, and others have used the phase change induced by optothermal actuation as a valving mechanism (see the review by Strohmeier *et al.*[3]). Here no phase change is involved but the bursting pressure is changed by changing the properties of the liquid. We show how the optically actuated valve can be used to dynamically capture a single particle by bursting the valve when the particle approaches it. The high flow induced by bursting the valve forces the bead through the constriction that then works as a hydrodynamic trap.

MATERIALS AND METHODS

The microfluidic device consists of microchannels defined at a single depth connecting capillary burst valves (Figure 1(a)) placed in parallel along the main channel (Figure 1(b)) accessible by Luer connectors. The microfluidic part was fabricated by injection moulding as described elsewhere[11] (Figure 1(c)). Briefly, a silicon master is fabricated by UV photolithography followed by a deep reactive ion etch that defines the microfluidic structures with a depth of 31 μm. A nickel replica of the silicon master is made, and the devices were injection molded in cyclic olefin copolymer (COC) (Topas 5013, TOPAS Advanced Polymers, Inc.) using a melt temperature of 250 °C, shim temperature of 155 °C, peak pressure of 1155 bars, and a demolding temperature of 135 °C.

a)rcwm@nanotech.dtu.dk

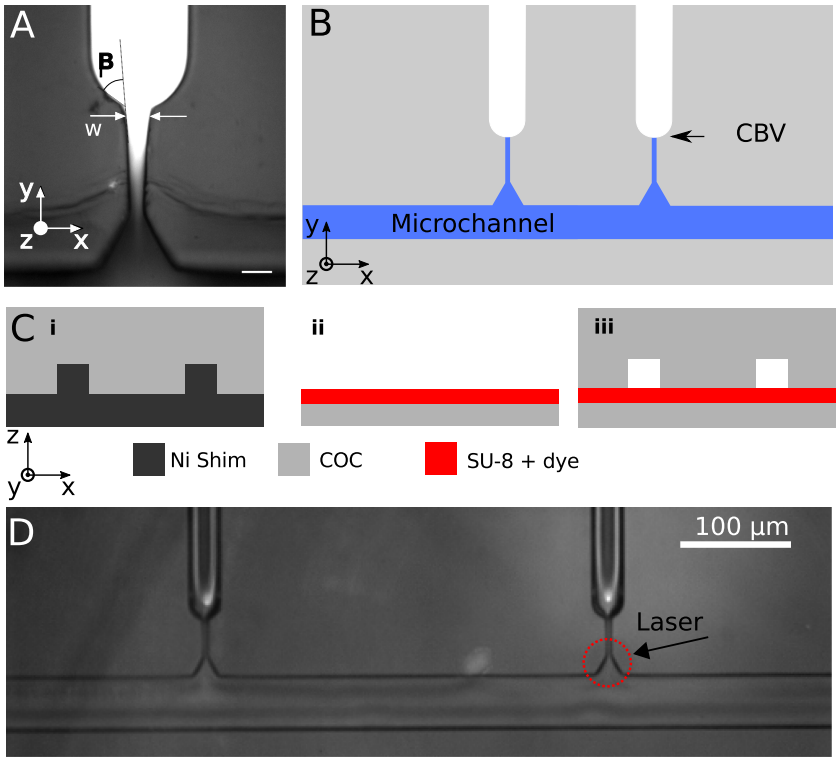

FIG. 1. (a) Planar capillary burst valve device before bonding with the lid. The scale bar is 10 μm. (b) Overall design of the device. (c) The three main steps of the fabrication process are as follows: (i) Injection moulding of the 31 μm-deep channels with a Ni shim. (ii) The lid is fabricated by spin coating an infrared absorber on a COC foil. (iii) UV-assisted thermal bonding of the injection moulded part and the lid. (d) Microscopy image of the device with the main channel filled with water and the outlet channels dry.

The channels were sealed with a lid using UV assisted bonding at 120 °C and a pressure of 51 bars for 5 min using a P/O/Weber press. The lid consists of a 500 μm-thick TOPAS 5013 foil coated with a layer of phthalocyanine dye (PROJET 800NP, Fujifilm) dissolved in the epoxy-based negative resist SU-8 (SU-8 2002, Microchem Corp.) (Figure 1(c)). First, a solution containing 14.5 wt. % SU-8 and 0.4 wt. % dye dissolved in pure cyclopentanone was prepared and spin coated on a 500 μm-thick foil. After a pre-exposure bake at 90 °C for 2 min, the thin film was flood exposed (EVG Aligner AL6-2) using a dose of 1500 mJ cm^{-2}. Then a postexposure bake at 90 °C for 2 min was carried out. The SU-8 layer was finally covered with a layer of TOPAS5013 dissolved in sec-butylbenzene. Prior to bonding, the polymer device and lid had been exposed to UV light from a mercury arc lamp for 30 s.

For optothermal actuation, we use the light of a 785 nm laser diode (Thorlabs) launched in a multimode fibre and focused on the optothermal actuation layer with a 50× objective (Thorlabs, NA = 0.45) from the back side of the device.[10] From the front side, through the lid, we image the chip in epi-fluorescence microscopy using an inverted microscope (Nikon Eclipse, Japan).

The LUER connectors are used as reservoirs containing up to 30 μl of solution. They are connected to a multi-channel pressure controller (MFCS-EZ, Fluigent), and pressures are set and measured from the provided software (Maesflo, Fluigent). The instrument provides a 0.3 mbar precision throughout the whole scale. For each measurement, the main channel is primed with the solution from one of the inlets, keeping the pressure on the outlet channels of the eight valves placed in parallel to prevent the CBVs from bursting at that stage. Initially all pressures are raised to 300 mbar. In order to measure the bursting pressure of an individual valve, the pressure at the outlet of the valve is reduced gradually until it bursts. We read the pressure drop between the main channel (300 mbar) and the outlet channel as the bursting pressure. As a consequence, there is no flow in the main channel during the measurement.

For trapping particles, 7 μm polymer beads are dispersed in a 0.01% Triton-X100 solution. The bead concentration is kept low so that single particles are travelling the main channel at a time. A flow in the main channel is maintained by lowering the pressure at one of the inlets while keeping the main channel at a pressure below the room temperature bursting pressure but above the burst pressure at 60 °C. This ensures that when the temperature rises, the valve burst and solution flows toward the outlet.

RESULTS AND DISCUSSION

The bursting pressure of a capillary burst valve depends on the surface tension of the liquid, the contact angle, and the change of angle of the channel wall at the valve.[4] For a cylindrical channel,

$$\Delta P = -4\gamma \frac{cos\,(\theta_a + \beta)}{D}, \tag{1}$$

where γ is the surface tension, θ_a is the advancing contact angle of the solution, β is the change of angle at the valve, and D is the channel diameter. For a rectangular channel,

$$\Delta P = -2\gamma \left[\frac{cos\,(\theta_a + \beta)}{w} + \frac{cos\,\theta_a}{h} \right], \tag{2}$$

where w is the channel width and h is the height. At the valve, the channel width changes abruptly with an angle β (see the supplementary material). In principle, the surface tension and the contact angle are both influenced by temperature. However,

the temperature dependence of the contact angle is small in many cases.[12] The surface tension γ on the contrary is known to have an almost linear temperature dependence in the range 20–70 °C considered here[13] so that we can expect the burst pressure to decrease linearly when the temperature increases (see the supplementary material).

We design a capillary burst valve with a planar design at a fixed depth of $h = 31$ μm (Figure 1(a)). The device is a microfluidic channel where a constriction constituting the capillary burst valve connects the main channel to separated outlet channels (Figure 1(b)). Due to a local reactive ion etch effect, the depth of the constriction itself is as low as 22 μm but the meniscus is pinned at the exit of the valve where the depth is the nominal depth. Microfluidic channels are fabricated in Cyclic Olefin Copolymer (COC) using injection moulding and assembled with a lid using UV-assisted thermal bonding[14] (Figure 1(c)). The optothermal actuation layer is included in the lid of the device that is a 500 μm COC foil coated with a ~300 nm layer of SU-8 functionalized with an absorber dye and finally coated with a layer of COC for promoting UV-assisted thermal bonding. Figure 1(d) shows a bonded device with the main channel wet and two capillary burst valves leading to individual dry outlet channels. In order to ensure a good separation of the nickel shim from the replicated polymer microfluidic device during injection moulding, the channels' side walls have a positive slope of ~3° such that channels are wider at the top. The cross section of the constriction is therefore trapezoidal with the width w of 7.4 μm and 4.5 μm at the top and bottom, respectively, measured after bonding with the lid. We measure the angle β to be 60°.

We test our device with pure water and a 0.01% solution of Triton-X100, a nonionic surfactant used in microfluidics made of COC to prevent stiction. In our device, the bursting pressure is 225 mbar and 60 mbar, respectively, for pure water and a 0.01% Triton-X100 solution (Figure 2). The bursting pressures of the valve agree well, considering the chip-to-chip variation, with values (234 mbar and 55 mbar for pure water and Triton-X100 solution, respectively) calculated using

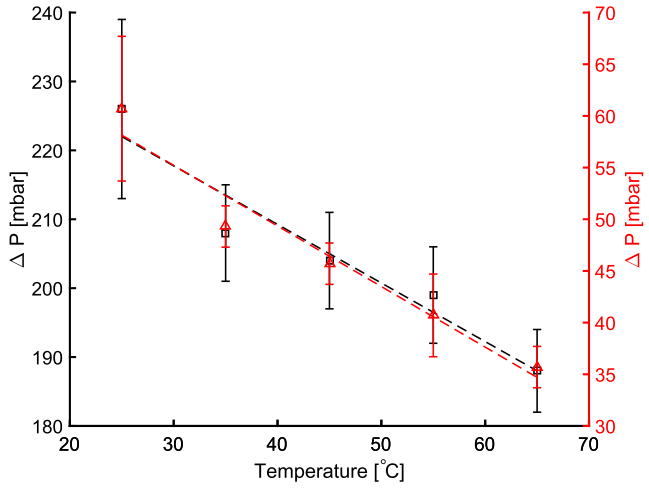

FIG. 2. Burst pressure as a function of the temperature for deionised water (squares, left axis) and a 0.01% solution of Triton-X100 in deionised water (triangles, right axis). The burst pressure is measured on several traps of different devices at each temperature. Error bars are the standard error on the mean. Linear fit for each solution is shown (dashed lines).

Equation (2) with $w = 5.9$ μm and $\beta = 60°$. For water, the advancing contact angle on TOPAS 5013 is 99°.[15] The surface tension is 72 mN m^{-1} at 25 °C. For the 0.01% Triton-X100 solution, we measure $\theta = 66°$ as the advancing contact angle. The surface tension at 25 °C is reported to be 32 mN m^{-1} by Gobel and Joppien.[16]

Equation (2) assumes (i) a sharp change of angle of the micro channel side wall at the valve and (ii) a rectangular cross section for the channel. Fabrication issues may challenge both assumptions. First, there is a rounding of the side wall at the valve which may produce a lower effective angle β as pointed out by Cho *et al.*[4] and calculated by Hagmeyer *et al.*[7] The rounding is due to two main steps in the fabrication process. During the fabrication of the nickel shim, microchannels are etched in silicon through a photoresist mask which may reflow during processing.[4] During the replication of the Ni shim by injection molding, additional rounding may be obtained. Second, the fabrication by injection moulding also implies a positive slope of the channel walls. Consequently, the meniscus at the valve has a base with a trapezoidal shape such that in our calculation we use an effective width of the constriction $w = 5.9$ μm that is the average of the width at the top and the bottom of the channel. We record the bursting pressure of individual valves at increasing chip temperature. We measure a temperature dependence of -0.85 ± 0.42 and -0.58 ± 0.23 mbar K^{-1} for water and Triton-X100, respectively, in agreement with the expected temperature dependence of the surface tension (–0.43 mbar K^{-1}).

Next, we make use of the optothermal actuation to raise the temperature of individual valves by focusing an infra-red laser (wavelength 785 nm, power <40 mW CW) on the lid in the vicinity or above the valve of interest. The optothermal actuation layer is embedded in the lid and has an absorbance of 69% (see the supplementary material). We have previously shown, using imaging of a temperature dependent fluorescent dye, that the laser spot diameter is 5 μm[10] and typically produces a temperature rise with a stretched exponential profile and a FWHM of 7 μm within a few hundreds nanometers from the absorber layer itself (see the supplementary information in Ref. 17). At high power, the optothermal actuation is able to locally raise the temperature such that the polymer melts.[10] At lower power, the temperature of the solution in the microfluidic channel can be evaporated. At even lower power, we have also shown that the temperature increase can be adjusted to induce a phase transition of a thermally actuated hydrogel at ~30 °C.[18] Since increasing the temperature to 60 °C is sufficient to induce a bursting pressure change larger than the chip-to-chip variation at room temperature, we hypothesize that the power of the actuating laser can be adjusted to yield a temperature rise sufficient to burst the valves (Figure 2) without inducing boiling of the solution or even denaturating proteins. To achieve bursting at the onset of the laser, we first apply a pressure across the valve that is just below the bursting pressure at room temperature. We adjust the laser power such that the temperature of the liquid at the valve rises sufficiently for the bursting pressure to drop below the set pressure. We achieve this condition for a diode current of 80 mA corresponding to ≈14 mW absorbed in the actuation layer at the laser spot (see the supplementary material). Indeed, the valve bursts at the

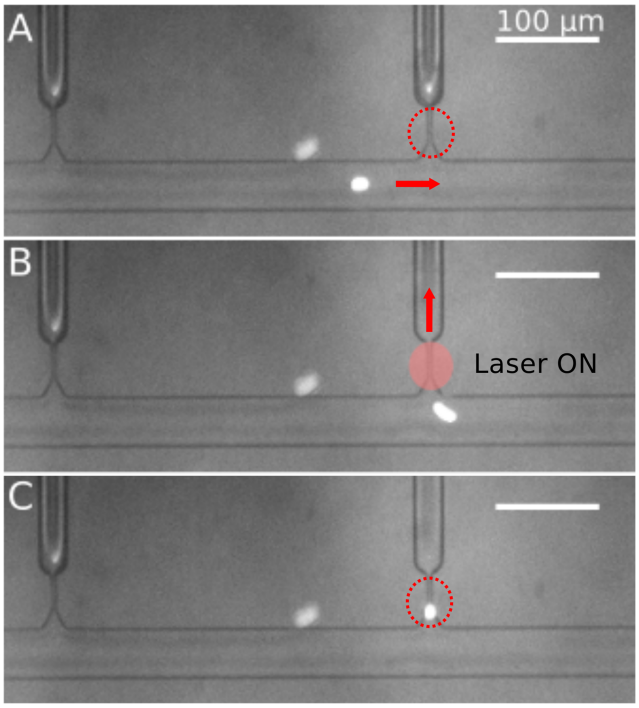

FIG. 3. Fluorescence and bright field microscopy images showing the capture of a single polystyrene bead. (a) A polystyrene bead is moving into the field of view from left. (b) The laser is turned on when the bead is in the vicinity of the valve that bursts and induces a flow through the valve. (c) The bead is captured at the valve due to the flow constriction.

onset of the laser, and the liquid fills instantaneously the outlet channel.

Optically actuated microvalves have several applications in centrifugal microfluidics.[19] Here we demonstrate how the optothermally actuated capillary burst valve can be used to trap single particles using the valve as a particle trap. The capillary burst valve is essentially a microfluidic constriction that we use for the hydrodynamic trapping of 7 μm fluorescent polymer beads. As a single bead passes in the main channel in the vicinity of the valve (Figure 3(a)), the laser is turned on and the valve bursts inducing a large flow through the constriction. The bead is dragged into the constriction and captured (Figure 3(b)). In this experiment, the trapped particle is a hard sphere such that the particle trap can be used for any particle with a diameter larger than the trap width; however, hydrodynamic traps have been used to trap deformable particles such as cells.[19–22] In the case of a deformable particle, the flow velocity through the constriction must be adjusted; thus the trapped particle is not flushed through the constriction. In our design, this could be achieved by decreasing the cross-sectional area of the outlet channel or introducing a second capillary burst valve in series in order to, respectively, limit the flow velocity and the volume of solution passing through the valve once burst. Notably, limiting the volume of solution that passes through the trap is a way to ensure that a single particle gets trapped when the bead concentration is higher than in our experiment and multiple particles are in the vicinity of the trap.

SUPPLEMENTARY MATERIAL

See supplementary material for the calculation of the bursting pressure at a different rounding of the valve edge and for different temperatures. It also includes measurements of the optothermal actuation film absorbance.

ACKNOWLEDGMENTS

The authors gratefully acknowledge funding from the European Commission under the Seventh Framework Programme (No. FP7/2007-2013) under Grant Agreement No. 278204 (Cellomatic).

[1] M. A. Unger, H. P. Chou, T. Thorsen, A. Scherer, and S. R. Quake, Science **288**, 113 (2000).
[2] R. Burger, D. Kirby, M. Glynn, C. Nwankire, M. O'Sullivan, J. Siegrist, D. Kinahan, G. Aguirre, G. Kijanka, R. A. Gorkin, and J. Ducree, Curr. Opin. Chem. Biol. **16**, 409 (2012).
[3] O. Strohmeier, M. Keller, F. Schwemmer, S. Zehnle, D. Mark, F. von Stetten, R. Zengerle, and N. Paust, Chem. Soc. Rev. **44**, 6187 (2015).
[4] H. Cho, H.-Y. Kim, J. Y. Kang, and T. S. Kim, J. Colloid Interface Sci. **306**, 379 (2007).
[5] A. L. Vig, K. Haldrup, N. B. Enevoldsen, A. H. Thilsted, J. Eriksen, A. Kristensen, R. K. Feidenhans, and M. M. Nielsen, Rev. Sci. Instrum. **80**, 115114 (2009).
[6] P. Vulto, S. Podszun, P. Meyer, C. Hermann, A. Manz, and G. A. Urban, Lab Chip **11**, 1596 (2011).
[7] B. Hagmeyer, F. Zechnall, and M. Stelzle, Biomicrofluidics **8**, 056501 (2014).
[8] R. Safavieh and D. Juncker, Lab Chip **13**, 4180 (2013).
[9] D. Duffy, H. Gillis, J. Lin, N. Sheppard, and G. Kellogg, Anal. Chem. **71**, 4669 (1999).
[10] L. H. Thamdrup, N. B. Larsen, and A. Kristensen, Nano Lett. **10**, 826 (2010).
[11] M. P. Jensen, N. Ashley, K. Koprowska, K. U. Mir, M. Zalkovskij, B. Bilenberg, W. Bodmer, A. Kristensen, and R. Marie, Lab Chip **15**, 4598 (2015).
[12] M. Phillips and A. Riddifor, Nature **205**, 1005 (1965).
[13] N. B. Vargaftik, B. N. Volkov, and L. D. Voljak, J. Phys. Chem. Ref. Data **12**, 817 (1983).
[14] P. Utko, F. Persson, A. Kristensen, and N. B. Larsen, Lab Chip **11**, 303 (2011).
[15] D. Mark, T. Metz, S. Haeberle, S. Lutz, J. Ducree, R. Zengerle, and F. von Stetten, Lab Chip **9**, 3599 (2009).
[16] J. Gobel and G. Joppien, J. Colloid Interface Sci. **191**, 30 (1997).
[17] J. N. Pedersen, C. J. Luscher, R. Marie, L. H. Thamdrup, A. Kristensen, and H. Flyvbjerg, Phys. Rev. Lett. **113**, 268301 (2014).
[18] J. Eriksen, A. H. Thilsted, R. Marie, C. J. Luscher, L. B. Nielsen, W. E. Svendsen, P. Szabo, and A. Kristensen, Biomicrofluidics **5**, 031101 (2011).
[19] R. Burger, D. Kurzbuch, R. Gorkin, G. Kijanka, M. Glynn, C. McDonagh, and J. Ducree, Lab Chip **15**, 378 (2015).
[20] Z. Wang, M.-C. Kim, M. Marquez, and T. Thorsen, Lab Chip **7**, 740 (2007).
[21] S. Kobel, A. Valero, J. Latt, P. Renaud, and M. Lutolf, Lab Chip **10**, 857 (2010).
[22] W.-H. Tan and S. Takeuchi, Lab Chip **8**, 259 (2008).